The Role of Matrix Stiffness in the Regulation of Matrix Metalloproteinase Activity

Bachelors of Science Honors Thesis

Presented in Partial Fulfillment of the Requirements for Graduation with Distinction in Biomedical Engineering from The Ohio State University

By

Kathryn Kaltenmark

The Ohio State University

May 2017

Honors Thesis Committee:

Dr. Jennifer Leight, Advisor

Dr. Tanya Nocera

Acknowledgements:

I would like to thank Dr. Jennifer Leight for her mentorship and guidance over these past three years. Dr. Leight has been my role model, has continuously supported all of my research endeavors, and has encouraged me to pursue my dreams. I am grateful for the countless hours Dr. Leight has invested into my education and growth as a researcher and biomedical engineer. My time spent on this project and the independence I was granted by Dr. Leight have allowed me to learn a wide variety of techniques and life lessons that have strengthened me as an undergraduate and will benefit me as I pursue a career in medicine. I am grateful for the opportunity to work with Dr. Leight, for the lessons I have learned from this project, and for the incredible experiences I have gained with her support.

The members of the Leight lab have also been supportive of me throughout this project. I would like to thank Jessica for her guidance, support, and advice over these past two and a half years. She helped me in developing the in situ zymography technique at the start of this project and has been a great teacher as well as a source of advice and encouragement throughout this project. My time in this lab would not have been the same without her. I would also like to thank Tori for her support and encouragement throughout this project. We both began in the Leight lab at the same time, and it has been great to have her as a companion and role model throughout this time. I would also like to thank Caitlin for her support, guidance, and for being a resource during this project. I would also like to thank Ameya and Abdul for their support, encouragement, and feedback throughout this project.

I would also like to thank my parents. I would not have been able to complete this project without their unconditional love and support. I would also like to thank my family and friends for their support, encouragement, and for helping me maintain balance in my life.

Abstract

Matrix metalloproteinases (MMPs) are a family of proteolytic enzymes that enable cell-mediated remodeling of the tumor microenvironment. MMP levels have been found to be upregulated in almost all tumor types and have been shown to play a critical role in extracellular matrix remodeling, basement membrane penetration, and eventually, tumor metastasis. It has been shown that matrix stiffness increases with tumor progression, however, it has yet to be elucidated how mechanical cues from the microenvironment such as matrix stiffness work to regulate MMP activity and how this activity is spatially distributed. Recently, a mouse model has been developed which recapitulates the malignant transformation of mammary epithelial tumors attributed to increased collagen and extracellular matrix (ECM) deposition by stromal fibroblasts which is associated with increased tumor incidence and load. We hypothesized that the increased matrix stiffness associated with tumor progression will enhance MMP activity of stromal fibroblasts. To investigate this hypothesis, we utilized a poly(ethylene glycol) hydrogel system functionalized with a fluorogenic MMP sensor to pursue two aims: 1) visualization and quantification of in situ MMP activity in murine mammary tumors and 2) encapsulation of isolated fibroblasts in hydrogels with precisely tuned stiffness. Results investigating the effect of matrix stiffness on MMP activity of isolated fibroblasts indicate no significant relationship due to large variability between experiments. In situ zymography experiments showed specific localization of MMP activity on tissues that can be localized to specific cell types when combined with immunohistochemistry. A better understanding of the underlying mechanisms of the tumor microenvironment will help lead to more effective cancer therapeutics.

Table of Contents

List of Figures

List of Tables

List of Equations

1. Introduction - Matrix Metalloproteinases and Their Importance within the Tumor Microenvironment

Matrix metalloproteinases (MMPs) are a family of proteolytic enzymes composed of more than 20 members that work to degrade extracellular matrix (ECM) components (Verma et al, 2007). MMPs are involved in highly-regulated processes critical to both normal and pathological physiology (Beckstead et al, 1994). The collagenase family of MMPs including MMP-1, MMP-8, and MMP-13 are responsible for degrading interstitial collagen fibrils I, II, and III that compose the ECM (Beckstead et al, 1994). Normal turnover and remodeling of the ECM during embryogenesis, ovulation, bone growth and repair, and angiogenesis are due in part to the collagenase family of MMPs (Beckstead et al, 1994, Luke et al, 1999). MMP activity has been linked to pathological physiologies such as rheumatoid arthritis, periodontal disease, and tumor metastasis (Beckstead et al, 1994, Luke et al, 1999). Upregulated MMP activity has been seen in almost all tumor types, and MMPs have been found to play a critical role in tumor growth, basement membrane penetration, and eventually, tumor metastasis (Deryugina et al, 2006). How MMP activity is regulated within the tumor microenvironment has yet to be fully elucidated.

1.1 Background - Tissue Stiffness during Tumor Progression

Palpation is a common method for tumor screening and can be done by detecting more rigid tumor tissues within softer, more compliant normal tissue (Bryan et al, 2013). It has been shown that fibrotic stiff tumors are associated with poor prognosis (Colpaert et al, 2001). It is of critical importance to develop ways to study the tumor microenvironment to better understand molecular mechanisms behind tumor cell behavior. In studying tumor cell behavior, matching the microenvironment mechanics is important when creating in vitro and in vivo models. Recently, matrix stiffness was of normal and tumorous breast tissue was characterized by

quantifying the elastic moduli of murine mammary gland tissues (Paszek et al, 2005). In Figure 1-1, it is shown that normal murine mammary gland tissues have elastic moduli of 0.167 kPa whereas murine breast tumor tissues have an elastic modulus of 4.049 kPa (Paszek et al, 2005). Another study was performed on normal, tumor, and adjacent to the tumor tissue on mouse mammary glands that characterized the elastic modulus of these tissues to be about 0.2, 0.5, and 1.8 kPa respectively (Levental et al, 2009). This characterization of elastic moduli in normal and tumor tissues allows for more accurate synthesis of in vitro models.

Tissue or Material	Elastic Modulus (Pa)
Normal Mammary Gland	167 ± 31
Average Tumor (Ras, Myc, Her2/Neu)	4049 ± 938 **
Stroma Attached to Tumor (Ras, Her2/Neu)	918 ± 269 **
Reconstituted Basement Membrane	175 ± 37
Collagen (2.0 mg/ml)	328 ± 87
Collagen (4.0 mg/ml)	1589 ± 380
Plastic (polystyrene) (Callister et al., 2000)	2.78×10^9
Glass (soda-lime) (Callister et al., 2000)	69×10^9

** Mean $\pm$ SEM, $p<0.01$

Figure 1-1. Elastic Moduli of Normal and Tumorous Breast Tissues (Paszek et al, 2005).

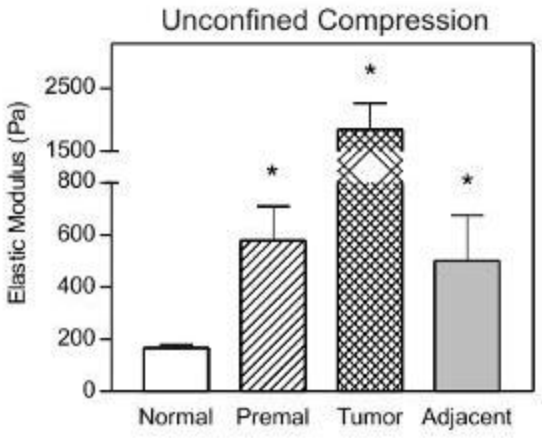

Figure 1-2. Elastic Moduli of Normal, Adjacent, and Tumor Tissues (Levental et al, 2009).(Levental Cell 2009)

The tumor microenvironment is composed of cells, numerous components secreted by cells including growth factors and cytokines, and many cross-linking proteins such as collagen and fibrin all orchestrated to create a dynamic microenvironment structure. To study the microenvironment, 3D in vitro models have been developed utilizing either native matrix components or by creating synthetic matrices via polymeric scaffolds. Native matrices include those composed of collagen, fibrin, reconstituted basement membrane, or cell-derived matrices (Leight et al, 2017). These matrices are beneficial in that they allow for studies of cell behavior in a biologically active environment focusing on ECM remodeling, morphogenesis, and stromal invasion and migration, however, these native matrices allow for limited control of elastic moduli, matrix architecture and matrix composition (Leight et al, 2017). Synthetic matrices have been developed utilizing polymers such as polyacrylamide, poly(ethylene-glycol) (PEG), and cross-linked hydrogels such as alginate and self-assembling peptides (Leight et al, 2017). These matrices can be fine-tuned to a wide range of stiffnesses and allow for in vitro studies of cell

migration, morphogenesis, and the independent control of material properties, however, integration of biological activity is limited (Leight et al, 2017).

The limited biological activity of synthetic matrices allows for studies of the isolation of microenvironment mechanics in regulating cell behavior. PEG-hydrogels are optimal in that they allow for maximal control of matrix stiffness, degradability, adhesive ligand presence, and control of spatial and temporal properties of the microenvironment (Leight et al, 2017). Recently, a fluorescently-labeled peptide biosensor was developed by Leight et al to quantify MMP activity in 3D PEG-hydrogels (Leight et al, 2013). The quenched, fluorescently-labeled biosensor is covalently-tethered to the 3D PEG-hydrogel matrix and MMP activity of encapsulated cells can be quantified upon cleavage of the peptide substrate by secreted active MMPs and the quantification of the resulting fluorescence (Leight et al, 2013). We proposed the use of this method in determining the role of matrix stiffness in regulating the MMP activity of murine fibroblast cells. PEG-hydrogels of stiffnesses ranging from 0.15-6.21 kPa were synthesized and fibroblasts isolated from both wildtype and Pten -/- murine mammary glands were encapsulated within the PEG-hydrogels. Covalently-tethered MMP-collagenase substrate was incorporated to allow quantification of MMP activity due to the collagenase family of MMPs. We hypothesized that tumor-associated murine mammary fibroblast cells would exhibit higher levels of MMP activity as tissue stiffness increases as compared to normal murine mammary fibroblast cells.

1.2 Background - In Situ Zymography to Localize MMP Activity of Tumor Microenvironment In Vitro

In situ zymography is a technique used to localize proteolytic MMP activity on histological tissue sections (George et al, 2010). This technique requires a fluorescently-labeled

native protein that is cleaved by active MMPs within the tissue allowing for MMP localization (George et al, 2010). Fluorescent substrates are either unquenched and MMP activity is localized by dark spots on a light background or substrates are quenched and MMP activity is localized by light spots on a dark background (George et al, 2010). Current MMP substrates are not easily modified to detect specific MMPs. A novel MMP biosensor was developed by Leight et al allowing for the easy exchange of the peptide backbone with quenched, coupled-fluorophores.

In situ zymography is performed using frozen tissue sections as this method preserves the endogenous MMP activity of the tissue which can be detected via MMP peptide substrates, however, this method compromises tissue morphology (Beckstead et al, 1994, George et al, 2010). Formalin-fixed tissue sections allow for excellent preservation of tissue morphology by cross-linking proteins and macromolecules within the microenvironment, however, this cross-linking action inhibits enzymatic activity and current MMP antibodies cannot accurately predict active MMPs due to interactions with MMP tissue inhibitors (Hadler-Olsen et al, 2010). Recently, this zinc-based fixative (ZBF) was used to fix murine normal kidney tissue using DQ gelatin to localize gelatinase and collagenase activity. Recently, a zinc-based fixative (ZBF) was developed that combines zinc salts including zinc-acetate and zinc-chloride in a tris buffer that was found to preserve endogenous enzymatic activity comparable to frozen tissue sections and preserve tissue morphology comparable to formalin-fixed tissue sections as seen in Figure 1-3 (Beckstead et al, 1994, Hadler-Olsen et al, 2010).

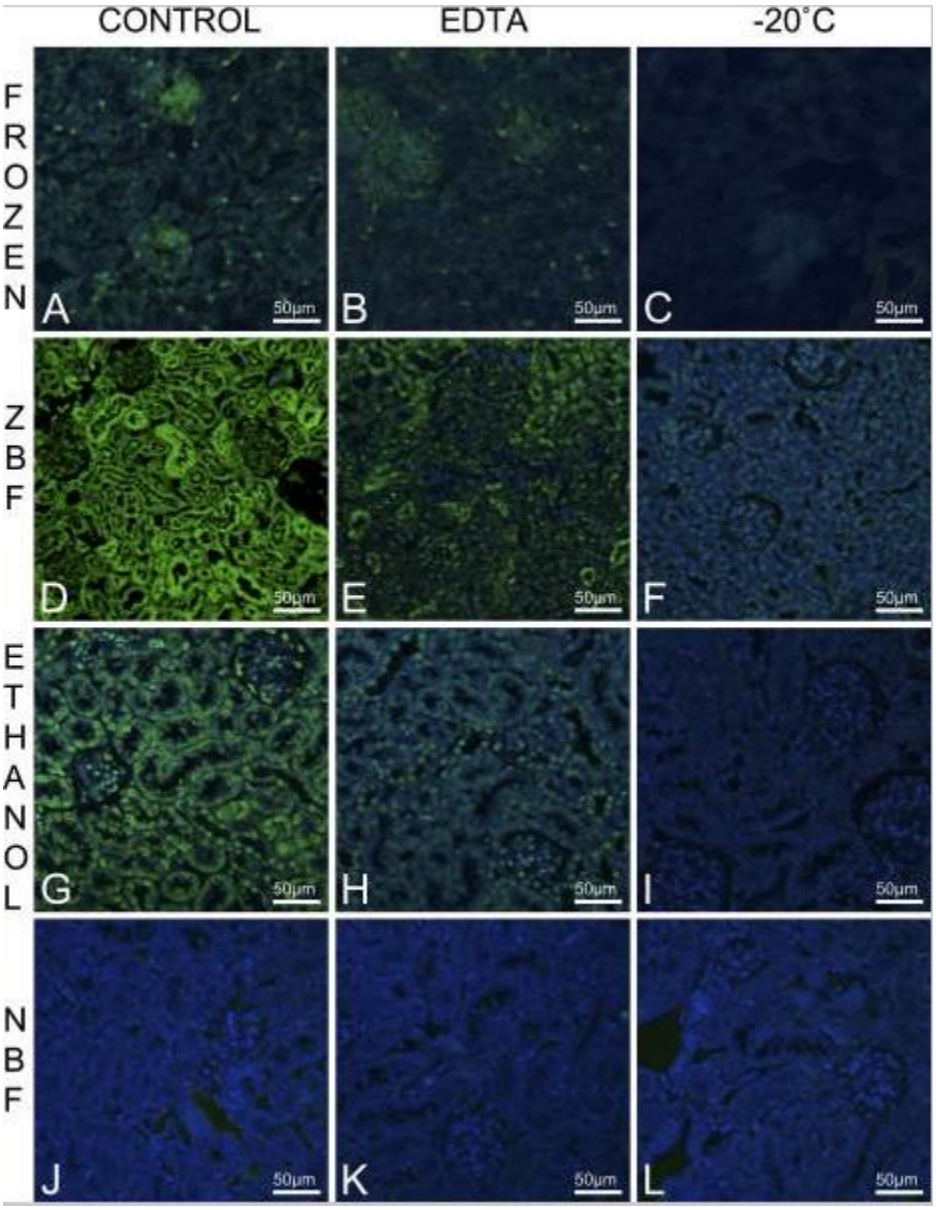

Figure 1-3. Comparison of Preservation of Enzymatic Activity and Tissue Morphology on Normal Murine Kidney Tissue Using Frozen, Zinc-Based, Ethanol, and Formalin Fixation Techniques (Hadler-Olsen et al).

We proposed a novel in situ zymography method using ZBF-fixed tissue sections in combination with a modular MMP-collagenase substrate developed by Leight et al allowing for

localization of specific MMP activity in situ. In situ zymography was performed in conjunction with immunohistochemistry to localize MMP activity to specific cell types allowing for a better understanding of MMP activity within the tumor microenvironment. This novel method was applied to murine melanoma skin tissues, murine wildtype and Pten -/- mammary tissues, and human pseudonormal, fibrous tumor-adjacent, and tumor breast tissues. We hypothesized that higher levels of MMP-collagenase activity will be observed in cancerous tissues as compared to normal tissues.

2. Materials and Methods

2.1 Synthesis of Fluorescently Labeled Peptide Biosensors

Collagenase peptide (Dab-GGPQG/IWGQK-Fl-AhxC) was synthesized using solid phase peptide synthesis on a Liberty BLUE Peptide Synthesizer (CEM) with a Rink Amide MBHA resin (Novabiochem). Fmoc protected amino acids were purchased from Chem-Impex. A dabcyl succinimidyl ester (Anaspec) was coupled on resin to the amino terminus in dimethyl formamide (DMF) with 6 equivalents of N,N'-diisopropylethylamine (DIPEA) and reacted overnight. Reaction completion was confirmed by a negative ninhydrin test. An orthogonally protected lysine (Lysine-Dde) (Chem-Impex) was deprotected two times using 2% hydrazine monohydrate in DMF for 10 minutes, and exposure of the free amine was confirmed by a positive ninhydrin test. Fluorescein NHS ester (Fisher Science) was coupled to the free amine as described for the dabcyl NHS ester. Peptides were cleaved from the resin using trifluoracetic acid (TFA), phenol, triisopropyl saline, water (95/2.5/1.25/1.25 v/v), allowed to react at room temperature for 4 hr, and precipitated three times in chilled diethyl ether. Peptides were purified by semi-preparative reverse phase high pressure liquid chromatography (Hitachi Elite La Chrom) using a 50-70% gradient of acetonitrile in water and expected mass of 1884 g/mol was confirmed by matrix assisted laser desorption ionization time-of-flight mass spectrometry (Bruker Ultrafle Xtreme).

2.2 Hydrogel Precursor Chemistry and Characterization

PEG-norbornene (PEG-NB) was synthesized from 4-arm PEG hydroxyl (Mn~20,000) or 8-arm PEG hydroxyl (Mn~20,000, Mn~40,000). (JenKe Technology USA) as described elsewhere (put in attached article). Briefly, 5-norbornene-2-carboxylic

acid (predominantly endo isomer; Alfa Aesar) was first converted to dinorbornene anhydride using N,N'-dicyclohexylcarbodiimide (0.5 eq. to norbornene; Sigma Aldrich) in dichloromethane. The 4-arm and 8-arm PEG monomers were then reacted overnight with the norbornene anhydride (5 eq. to PEG hydroxyls) in dichloromethane. Pyridine (5 eq. to PEG hydroxyls) and 4-dimethylaminopyridine (0.05 eq. to PEG hydroxyls) were also included. The reaction was conducted at room temperature under argon. End group functionalization was verified by 1H NMR. The photoinitiator lithium phenyl-2,4,6-trimethylbenzoylphosphinate (i.e., lithium acylphosphinate; LAP) was synthesized as described (attach included paper here). The peptide crosslinker, KCGPQG↑IWGQCK, and cell adhesion peptide, CRGDS, were purchased from American Peptide Company.

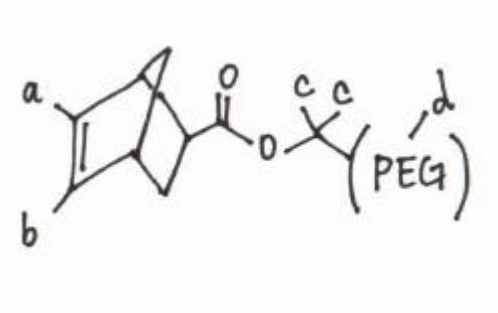

Figure 2-1 PEG-NB molecule with labeled hydrogens (a, b, c, d) analyzed by NMR. Number of hydrogens per norbornene (NB) group is given by "a + b" and the number of hydrogens per PEG arm is given by "d."

$$\#\ of\ hydrogens\ per\ PEG\ molecule\ arm$$
$$= (\#\ of\ end\ group\ hydrogens)(PEG\ molecular\ weight)$$
$$/(\#\ of\ hydrogens\ per\ PEG\ arm)(\#\ of\ PEG\ arms)$$

$$\#\ hydrogens\ per\ NB\ group\ (X) : \#\ of\ hydrogens\ per\ PEG\ molecule$$

Equation 2-1 Calculating the expected number of hydrogens per PEG molecule arm.

$$Percent\ functionalization$$
$$= \frac{(\#\ of\ hydrogens\ per\ NB\ group)(\#of\ expected\ hydrogens\ per\ PEG\ molecule\ arm)}{\#\ of\ hydrogens\ per\ PEG\ molecule\ arm}$$

Equation 2-2 Calculating the percent functionalization of NB per PEG arm.

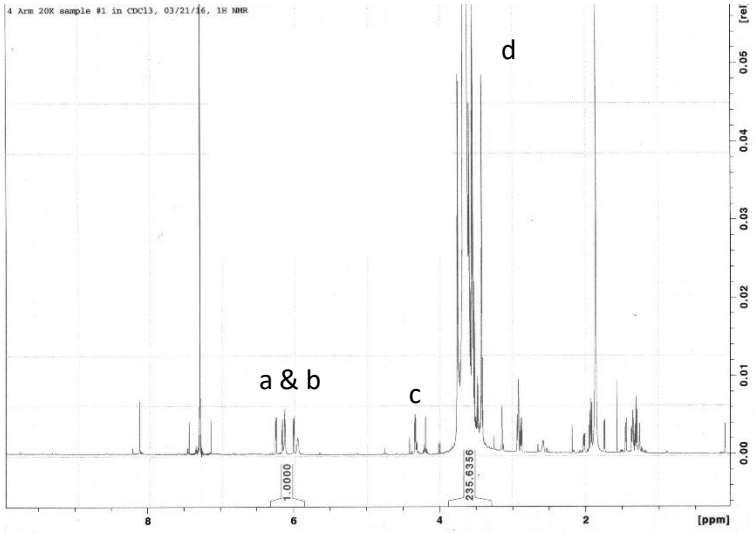

Figure 2-2. 4arm20k PEG-NB, 97% functionalized.

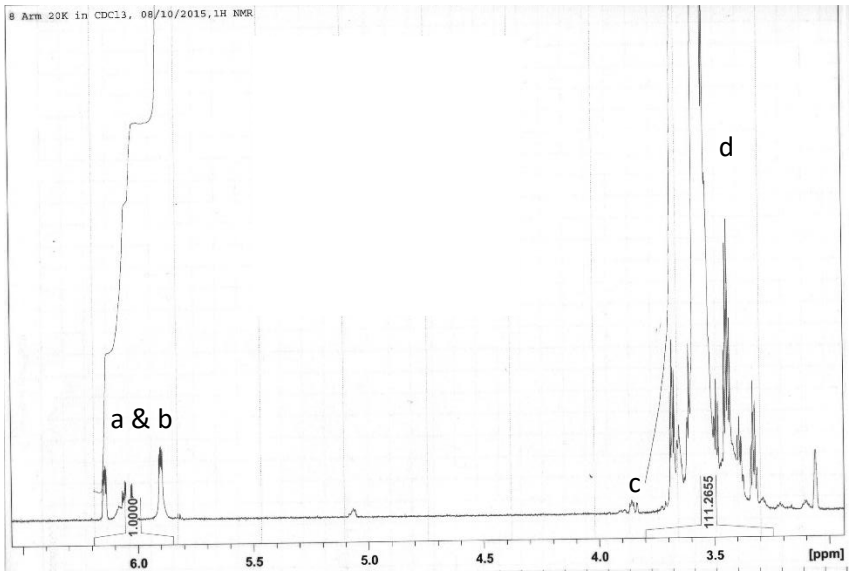

Figure 2-3. 8arm20k PEG-NB, 102% functionalized.

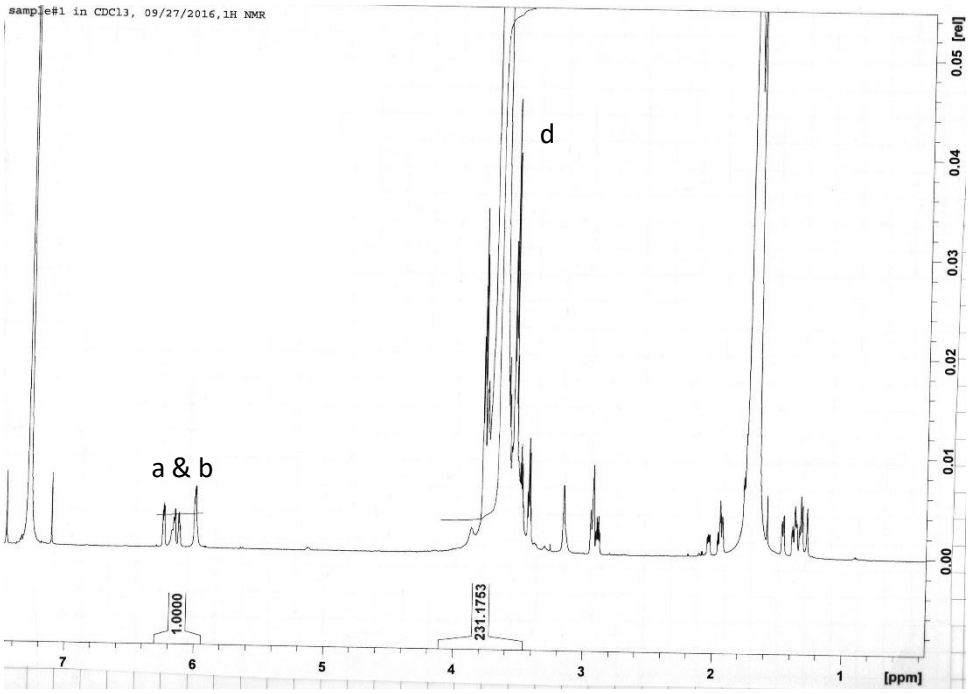

Figure 2-4. 8arm40k PEG-NB, 98% functionalized.

2.3 Cell Culture

Murine mammary fibroblast cells were isolated and donated by the Ostrowski lab. Cells were isolated from wildtype mice and mice with Pten-gene ablated mammary fibroblast cells. Pten is a part of the phosphoinositide 3-kinase pathway and has been shown to be a tumor suppressor gene (Trimboli et al, 2010). Knockdown of the Pten gene recapitulated increased stromal deposition by fibroblasts and was associated with increased mammary tumor incidence and load (Trimboli et al, 2010). Normal and tumor-associated murine mammary fibroblasts were cultured in high glucose phenol red Dulbecco's Modified Eagle Serum (HG DMEM) with 1% penicillin streptomycin, 1% L-glutamine, and 10% heat-inactivated fetal bovine serum. Cells were passaged up to passage 46 at 80% confluency using trypsin and washed using phosphate buffered saline.

For encapsulation experiments, HG DMEM with no phenol red, 1% penicillin streptomycin, 1% L-glutamine, and 1% charcoal-stripped serum.

2.4 Zinc-Based Tissue Fixation

Murine kidney, melanoma, and mammary gland tissues and human mammary tissues were fixed for 36-38 hr in zinc-based fixative (ZBF) containing 36.7 mM zinc-chloride, 27.3 mM zinc-acetate, and 0.63 mM calcium-acetate in 0.1 M Tris-HCl, pH 7.4 (Hadler-Olsen et al). The ZBF-fixed tissues were then paraffin embedded and 8 µm-thick sections were cut and placed on glass sides and used for further in situ zymography and immunohistochemistry stainings.

2.5 In Situ Zymography

ZBF-fixed, paraffin embedded 8 µm-thick serial tissue sections were obtained and either sat at room temperature for 60 minutes or placed in a dry oven at 55-60 ˚C for 20 minutes. Tissue sections were then deparaffinized and rehydrated in xylene and graded alcohol baths. Slides were placed in a xylene bath for 10 minutes, and then placed in a fresh xylene bath for 10 minutes. Slides were then immersed in 100% ethanol for 2 minutes, 95% ethanol for 1 minute, 70% ethanol for 1 minute, 50% ethanol for 1 minute, 30% ethanol for 1 minutes, 0.85% NaCl solution for 2 minutes, and phosphate buffered saline for 2 minutes.

Everything was protected from light. Conditions for in situ zymography included a -20 ˚C control, a +4 ˚C control, an unstained control, an experimental condition, and an MMP inhibitor control to control for effects on MMP activity due to temperature, autofluorescence of the tissue, active MMPs, and inactivated MMPs, respectively. The MMP inhibitor conditions were preincubated for 1 hr in inhibitor solutions (20 mM

EDTA or 100 µM phenanthroline in Milli-Q water) at 37 ˚C. Other conditions remained at room temperature. Peptide MMP biosensor substrate solutions were prepared at 50 µM collagenase peptide (Dab-GGPQG/IWGQK-Fl-AhxC) in reaction buffer containing 50 mM Tris-HCl, 150 mM NaCl, and 5 mM CaCl2. MMP inhibitor substrates were prepared at 200mM EDTA (Fisher Scientific) or 100 µM phenanthroline (Sigma Aldrich). After a 1 hr preincubation, MMP inhibitor conditions were coated with MMP inhibitor-modified peptide substrate solution, while the -20 ˚C control, a +4 ˚C control, and experimental conditions were coated with the unmodified peptide substrate solution. All conditions were incubated in humidified chambers at 37 ˚C except for control conditions which were incubated at -20 ˚C and +4 ˚C or at room temperature (unstained).

All slides were rinsed in Milli-Q water and fixed in 4% neutral buffered formalin for 10 minutes. Sections were then rinsed in phosphate buffered saline baths twice, and stained with Hoechst (Invitrogen) to counterstain nuclei at 2 µg/mL for 20 minutes. Slides were then mounted using ProLong Antifade Mountant (Life Technologies).

2.6 Immunohistochemistry

Everything was protected from light. After tissue fixation using 4% neutral buffered formalin, sections were permeabilized using 0.5% Tritin-X in PBS for 5 minutes. Sections were then blocked in 5% bovine serum albumin (BSA) in PBS for 1 hr at room temperature. Primary antibody solutions were prepared at 5µg/mL for monoclonal mouse anti-cytokeratin-8 (Developmental Studies Hybridoma Bank), monoclonal mouse anti-alpha-smooth muscle actin [1A4] (Sigma Aldrich) and monoclonal mouse anti-vimentin [V9] (Fisher Science) in 5% BSA in PBS. Sections were incubated for 1 hr at room temperature or overnight at +4˚C in humidity chambers.

After incubation, sections were rinsed three times with PBS. Secondary antibody solutions were prepared at 5 µg/mL using polyclonal goat anti-mouse Texas Red (ThermoFisher) and polyclonal goat anti-mouse Alexa Fluor 488 (Fisher Scientific) and at 2 µg/mL Hoechst (ThermoFisher) in 5% BSA in PBS. Sections were coated with the secondary antibody solutions and incubated for 1 hr at room temperature. Slides were then rinsed three times in PBS and mounted ProLong Antifade Mountant (ThermoFisher).

2.7 Microscopy

An Olympus FV 1000 spectral confocal microscope (Olympus Life Science) was used to image tissue samples stained by in situ zymography and immunohistochemistry. Experimental conditions were imaged first to obtain exposure times and brightness setting that were then used to take images of all other conditions to control for staining intensity. Images from individual experiments were taken on the same day. Images were taken at either 20x or 40x.

2.8 ImageJ Fluorescence Analysis

Quantification of fluorescence due to cleavage of the MMP peptide biosensor was calculated for in situ zymography stained murine ZBF-fixed kidney tissues by completing area scans of pixel intensity on MMP collagenase component images taken with the FITC channel. Three images were taken per condition and the average pixel intensity and standard error was calculated.

2.9 Thiolation of Glass Coverslips

Coverslips (12 mm, No. 1.5, Fisher Scientific) were thiolated via liquid deposition (0.5% (3-mercaptopropyl)trimethoxysilane (Sigma Aldrich)) in 95% ethanol/water solution for 3 minutes, rinsed in 95% ethanol/water, and dried at 80˚C.

2.10 Rheology

50 µL gels were polymerized in syringes, swollen in PBS overnight, and loaded onto a rheometer (Advanced Rheometer 2000ex, TA Instruments). 8 mm parallel plate geometry was used to measure the swollen gel modulus at 25˚C using a frequency sweep between 0.5 and 100 rad/s at an oscillatory strain of 0.5% and a gap size of 1100-2500 µm. Measurements were taken in the linear viscoelastic response regime.

2.11 PEG-Hydrogel Synthesis and Cell Encapsulation

3 mM (6 wt%) PEG-NB, MMP degradable crosslinker (KCGPQGIWGQCK), 0.5 mM CRGDS, 2 mM photoinitiator LAP, and 0.25 mM fluorogenic peptide substrate were mixed. Cells were encapsulated at a density of $4x10^6$ cells per mL in phosphate buffered saline. 50 µL gels were created by pipetting the PEG precursor-cell solution into silicone rubber gaskets on thiolated coverslips and polymerized using 365 nm light at an intensity of 4 mW/cm for 3 minutes. Post-encapsulation, gels were incubated in high-glucose no phenol red Dulbecco's Modified Eagle Serum with 1% penicillin streptomycin, 1% L-glutamine, and 1% charcoal-stripped fetal bovine serum for 24 hr.

2.12 Fluorescence Measurements

Fluorescence measurements were conducted with a SpectraMax M2 microplate reader (Molecular Devices), at 494 nm excitation (ex)/521 emission (em) for the fluorogenic peptide and 560 nm ex/590 nm em for alamarBlue (Life Technologies) with

21 points taken per well. Solution studies of peptide cleavage used 10 µM peptide and 20 µg/mL of 200 units/mg collagenase (Sigma Aldrich) or 20 µg/mL proteinase K (Sigma Aldrich) in phosphate buffered saline (pH 7.4). For studies with the fluorogenic peptides conjugated to PEG hydrogels and encapsulated cell experiments, an area scan was performed using a 24 well plate format.

2.13 Data Analysis

For hydrogel and in situ zymography data analysis, each experiment was performed at least three independent times with two replicates per condition. Data was analyzed with Graphpad Prism 7 software, using a two-way ANOVA with Bonferroni posttests or an unpaired student t-test. Statistical significance was determined when $p<0.05$.

3. Results and Discussion

3.1 Investigation of the Effects of Matrix Stiffness on MMP Activity in Murine Mammary Fibroblasts Encapsulated in PEG-Hydrogels

3.1.1 MMP Activity in Murine Mammary Fibroblasts Encapsulated in 4Arm20K PEG-hydrogels

As stated previously in section 2.3, murine mammary fibroblast cells were isolated and donated by the Ostrowski lab. Cells were isolated from wildtype mice and mice with Pten -/- mammary fibroblasts which were shown to be associated with malignant breast cancer phenotypes (Trimboli et al, 2010). To explore whether Pten -/- murine mammary fibroblasts exhibited higher MMP collagenase activity compared to wildtype murine mammary fibroblasts, the cells were encapsulated in 4Arm20K PEG-hydrogels with a PEG-NB to cross-linking ratio of

1:1 (thiol:enes) as seen in Figure 3.1. MMP collagenase activity normalized to cell viability as determined via Hoechst staining was found to be significantly higher (p=0.04638) in the Pten -/- fibroblast hydrogels than in the wildtype fibroblast hydrogels. In Pten -/- mouse models, the loss of Pten was found to increase MMP-9 activity among Pten -/- fibroblasts (Trimboli et al, 2010).

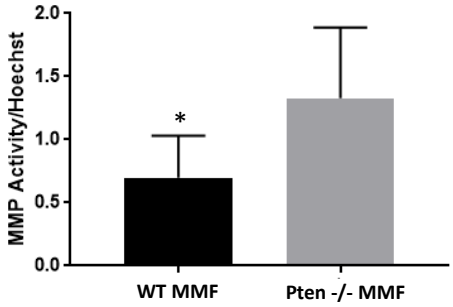

*Figure 3-1 Murine mammary fibroblast MMP activity/Hoechst (*p = 0.04638), n=4+SD.*

3.1.2 Rheology to Characterize Elastic Modulus of PEG-Hydrogels

PEG-hydrogels are viscoelastic materials meaning that they exhibit behavior of both elastic solids and viscous fluids. These properties are time-dependent and can be explored through rheology. PEG-hydrogels were first tested using a strain sweep as described in section 2.10 to measure the yielding behavior of the gel and verify that the gel testing parameters were in the linear regime and that the gels were expressing elastic solid behavior. A frequency sweep was then performed to verify the frequency independent characteristics of the gel and to determine the average storage modulus relating to the elastic modulus (stiffness) as seen in Equation 3-1. Stiffness was modulated by varying the molecular weight, number of arms, and by changing the crosslinking density of norbornene groups on PEG molecules to thiol groups on crosslinker peptides. The elastic modulus for 6 wt% PEG-NB hydrogels were determined for the following crosslinking ratios (thiol:enes) of 0.7, 0.85, and 1.

$$E_y = 2G_{yz}(1 + v_{yz})$$

Equation 3-1. Calculating Elastic Modulus from Storage Modulus (Pa).

E_y is the elastic modulus, G_{yz} is the storage modulus, and v_{yz} is Poisson's ratio equal to 0.5 assuming the gel is incompressible and deforms elastically at small strains.

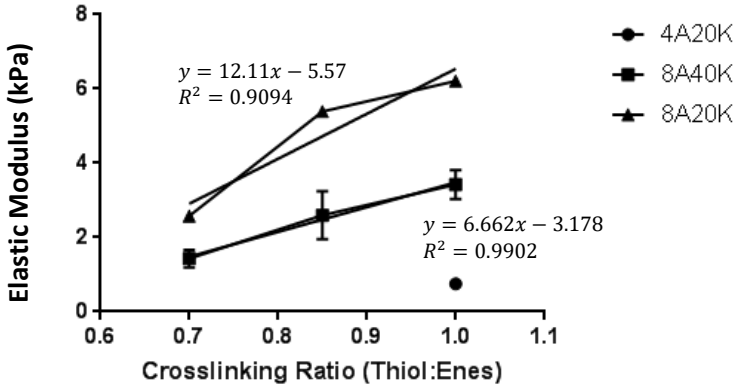

Figure 3-2 Moduli of 6 wt% PEG-hydrogels at varying crosslinking ratios, n=3+SD.

Crosslinking Density	4arm20k	8arm40k	8arm20k
0.70	-	1.42	2.58
0.85	-	2.60	5.39
1	0.75	3.43	6.21

Table 3-1 Elastic Moduli in kPa of PEG hydrogels of varying molecular weight and crosslinking density.

3.1.3 Encapsulating Murine Mammary Fibroblasts in PEG-hydrogels of Varying Stiffness

Tissue stiffness increases with tumor progression. To determine the effects of matrix stiffness on cell behavior, wildtype and Pten -/- murine mammary fibroblasts were encapsulated in PEG-hydrogels of stiffness ranging from 0.75-6.21 kPa. Stiffness conditions were chosen based on data presented by Levental et al (2009) characterizing the elastic moduli of normal, fibrous tissue adjacent to the tumor, and tumor tissues. MMP activity normalized to metabolic activity was not found to be statistically significant ($p=0.9836$) between wildtype and Pten -/- fibroblast conditions as seen in Figure 3-3. Upon analysis of metabolic activity of wildtype and Pten -/- mammary fibroblasts, a significant increase in metabolic activity across all stiffness conditions in the Pten -/- mammary fibroblasts as compared to the wildtype mammary fibroblasts was seen (Figure 3-4).

Although there was high variability of MMP activity normalized to metabolic activity (Figure 3-3), it was shown that cells remained viable and showed little variability in metabolic activity between experiments (Figure 3-4). We are not sure why there is large variability in MMP activity normalized to metabolic activity.

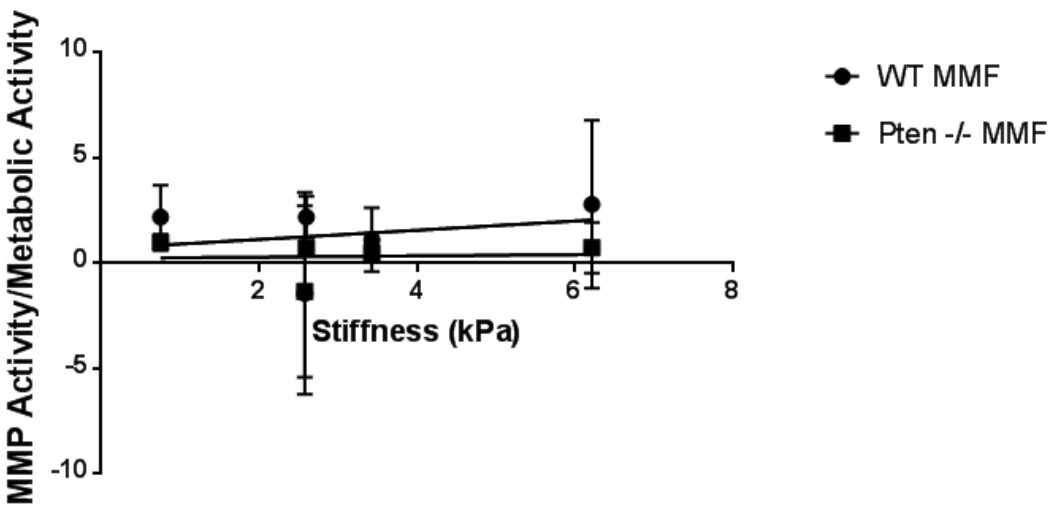

Figure 3-3 Normalized MMP activity/metabolic activity of wildtype and Pten -/- murine mammary fibroblasts in PEG-hydrogels of varying stiffness, n=4+SD.

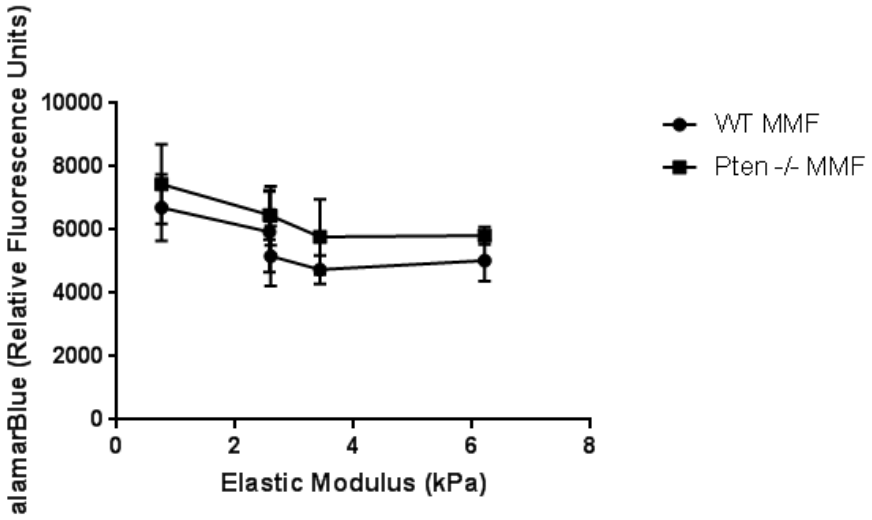

Figure 3-4. Metabolic activity of wildtype and Pten -/- murine mammary fibroblasts in PEG-hydrogels of varying stiffness, n=4+SD.

3.2 In Situ Zymography Optimization

3.2.1 Comparison of DQ Gelatin and MMP Collagenase Peptide

Hadler-Olsen et al (2010) showed that in situ zymography using a DQ gelatin substrate could be used to localize gelatinase and collagenase activity on ZBF-fixed tissues. It is unknown if this in situ zymography developed by Hadler-Olsen et al (2010) could be used with the MMP collagenase substrate developed by Leight et al (2013) in order to localize MMP activity.

In situ zymography using the quenched MMP collagenase peptide substrate developed by Leight et al was optimized according to the methods outlined by Hadler-Olsen et al (2010). ZBF-fixed murine kidney tissues were chosen for their homogeneous morphology. DQ-gelatin, a known gelatinase/collagenase substrate, showed similar fluorescent intensity related to protease activity as measured by the quenched MMP-collagenase substrate as seen in Figure 3-5.

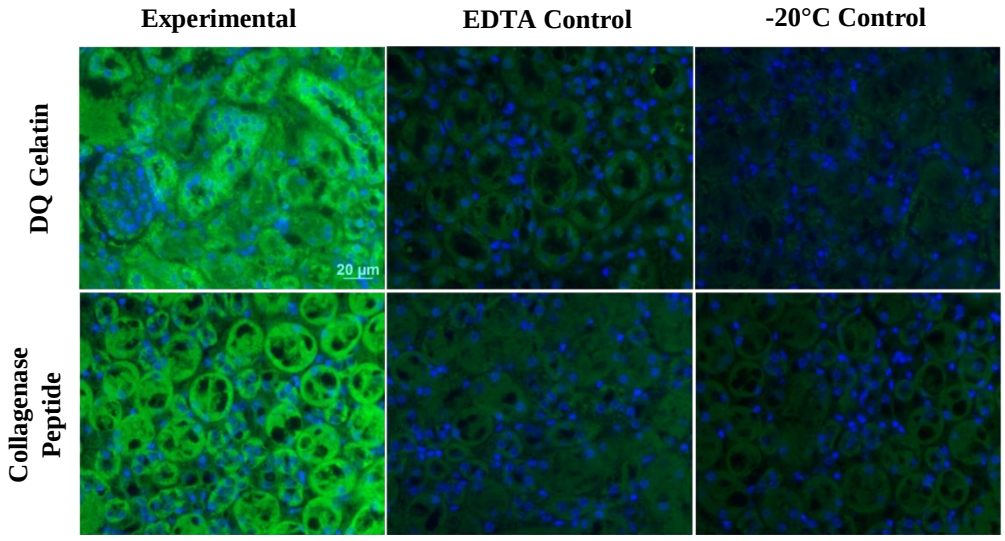

Figure 3-5 Fixed mouse kidney sections incubated with DQ gelatin and collagenase MMP fluorogenic sensor (green) and the DNA dye, Hoechst (blue), n=1. Images taken at 40x.

To control for MMP activity, a known zinc-ion chelator EDTA was used to sequester the Zn2+ ion from the MMP active site (Nyborg et al). EDTA is shown in Figure 3-6 and its mechanism for sequestering metal ions is shown in Figure 3-7. In situ zymography results showed a decrease in MMP activity when using the quenched MMP-collagenase substrate that was comparable to the results observed when using the DQ-gelatin substrate as seen in Figure 3-5.

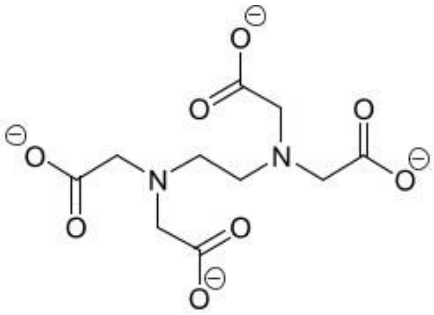

Figure 3-6 EDTA chemical structure (National Center for Biotechnology Information).

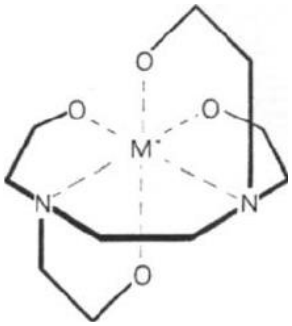

Figure 3-7 EDTA metal chelate (Goh et al, 2013).

Temperature controls were also included as MMP activity occurs within the body at 37˚C. A -20 ˚C control was included and results showed a significant decrease in MMP

activity as compared to the experimental condition. Results between the DQ-gelatin substrate and MMP-collagenase substrate were comparable as seen in Figure 3-5.

These results indicate that the in situ zymography method developed by Hadler-Olsen et al (2010) can be used with the MMP-collagenase peptide substrate developed by Leight et al (2013).

3.2.2 Optimization of Controls for In Situ Zymography

Previous optimization of the in situ zymography technique showed that the MMP collagenase substrate developed by Leight et al (2013) was compatible with the in situ zymography technique developed by Hadler-Olsen et al (2010). To better control for fluorescence detected due to MMP activity of the tissue cleaving the fluorogenic substrate, controls were further developed for in situ zymography. Unstained controls were introduced to control for autofluorescence of the tissue. A known MMP-inhibitor, phenanthroline, was optimized as a control for active MMP activity at 100 µM. Phenanthroline (Figure 3-8) is a metal chelator that inhibits MMP activity by sequestering the zinc-ion (Figure 3-9) from the MMP active site via the formation of a coordination complex (NCBI).

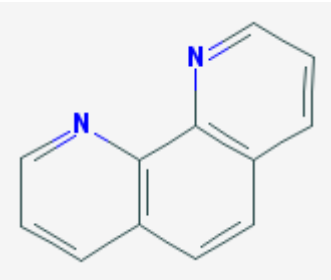

Figure 3-8 Phenanthroline Chemical Structure (NCBI).

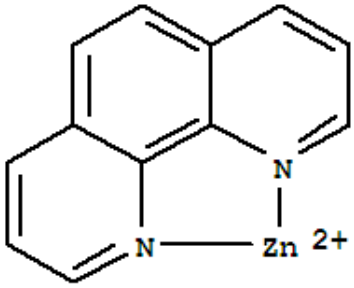

Figure 3-9 Phenanthroline Chelate with Zinc-ion (Guidechem).

Images from in situ zymography performed with the MMP-collagenase substrate as seen in Figure 3-10 were analyzed for fluorescent intensity using ImageJ software on FITC component images. Results showed that MMP-collagenase activity was significantly inhibited in all control conditions (Figure 3-11), proving the effectiveness of the controls and reliability of using the MMP-collagenase substrate to detect MMP activity via in situ zymography.

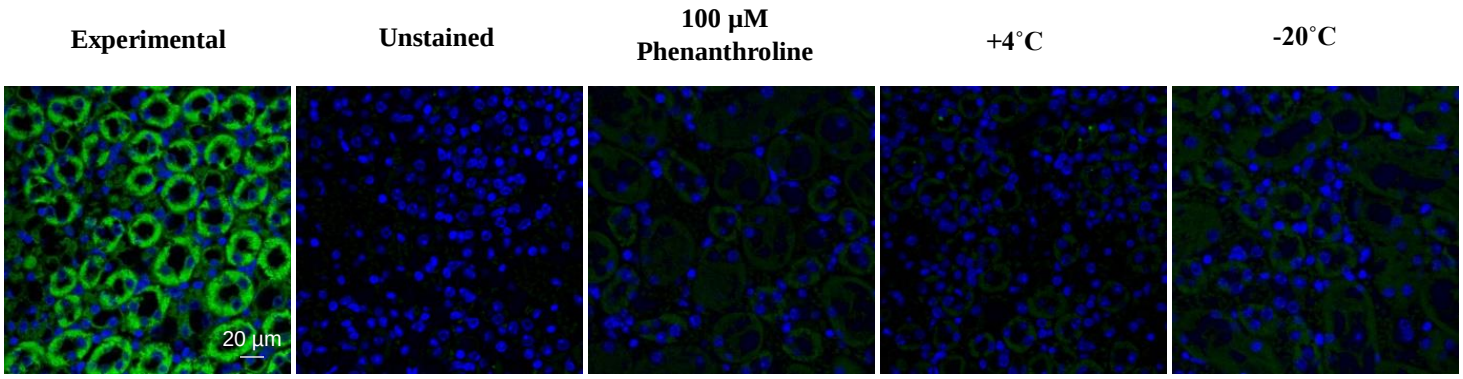

Figure 3-10 ZBF-fixed murine kidney tissue stained for MMP-collagenase (green) and the DNA-dye Hoechst (blue), n=4. Images taken at 40x.

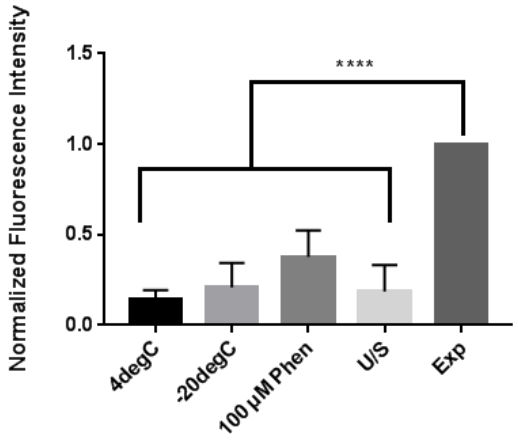

*Figure 3-11 ZBF-fixed controls for in situ zymography staining, n=4+SD. **** = p <0.0001*

3.2.3 Localization of MMP Collagenase Activity on Mouse Melanoma and Ability to Perform Immunohistochemistry after In Situ Zymography

Immunohistochemistry is a method for detecting antigens in cells of tissue sections by using antibodies binding for specific antigens in biological tissues (Duraiyan et al, 2012). The combination of immunohistochemistry and in situ zymography would allow for localization of MMP activity to specific cell types. It was shown that immunohistochemistry could be combined with in situ zymography after staining for MMP collagenase and vimentin in mouse melanoma tissue. Vimentin is an intermediate filament that is present in most mesenchymal cells and is found in almost all melanomas (Painter et al, 2010). Presence of vimentin immunohistochemical staining as well as MMP-collagenase in situ zymography staining shows the compatibility of these two methods (Figure 3-12).

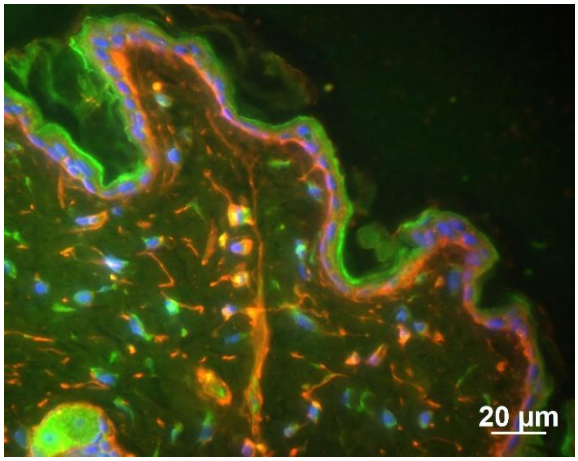

Figure 3-12 Fixed mouse melanoma section incubated with collagenase MMP fluorogenic sensor (green), the DNA dye, Hoechst (blue), and vimentin (red), n=1. Image taken at 40x.

3.2.4 Localization of MMP Collagenase Activity on Murine Mammary Glands

To spatially localize MMP-collagenase activity in vitro on both wildtype and Pten -/- mammary glands, glands were stained for MMP collagenase activity and Hoechst. Wildtype murine mammary glands were seen to have lesser cell density and more sparse MMP activity than Pten -/- mammary glands whose cell density was much higher and greater MMP activity throughout the tissue. These results agree with increased stromal deposition described by Trimboli et al.

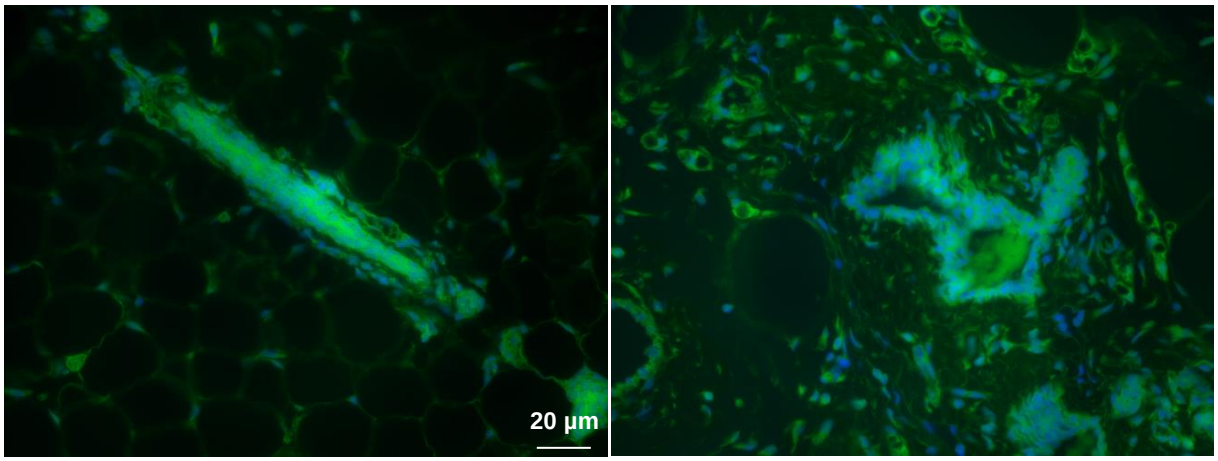

Figure 3-13 ZBF-fixed normal (right) and tumor-associated (left) murine mammary glands stained for MMP collagenase (green) and the DNA dye, Hoechst (blue), n=1. Image taken at 40x.

3.2.5 Localization of MMP Collagenase Activity on Human Breast Tissue in Combination with Immunohistochemistry

Many cells within the tumor microenvironment secrete MMPs including fibroblasts, macrophages, adipocytes, and epithelial cells. To observe epithelial cell structure and MMP collagenase activity in vitro, ZBF-fixed human breast tissues were stained for MMP collagenase activity using in situ zymography with the MMP-collagenase peptide biosensor followed by immunohistochemical staining of epithelial cells using the cytokeratin-8 antibody. Controls with and without primary antibody stainings were used to determine secondary antibody specificity. Pseudonormal and fibrous tissue adjacent to the tumor showed similar morphology and MMP-collagenase localization. In these tissues, epithelial ducts had a normal, cylindrical cross-section structure and were surrounded by organized fibrous stroma. Greater MMP activity levels were localized around the epithelial ducts with relatively moderate MMP activity levels localized to the fibrous stroma. In the patient's tumor tissue, disorganized epithelial

structures were observed. Greater MMP activity levels in tumor tissues were seen throughout the tissue. These observations correlate with disorganized epithelium and upregulated MMP levels found in breast tumors in the literature (Radisky et al, 2010).

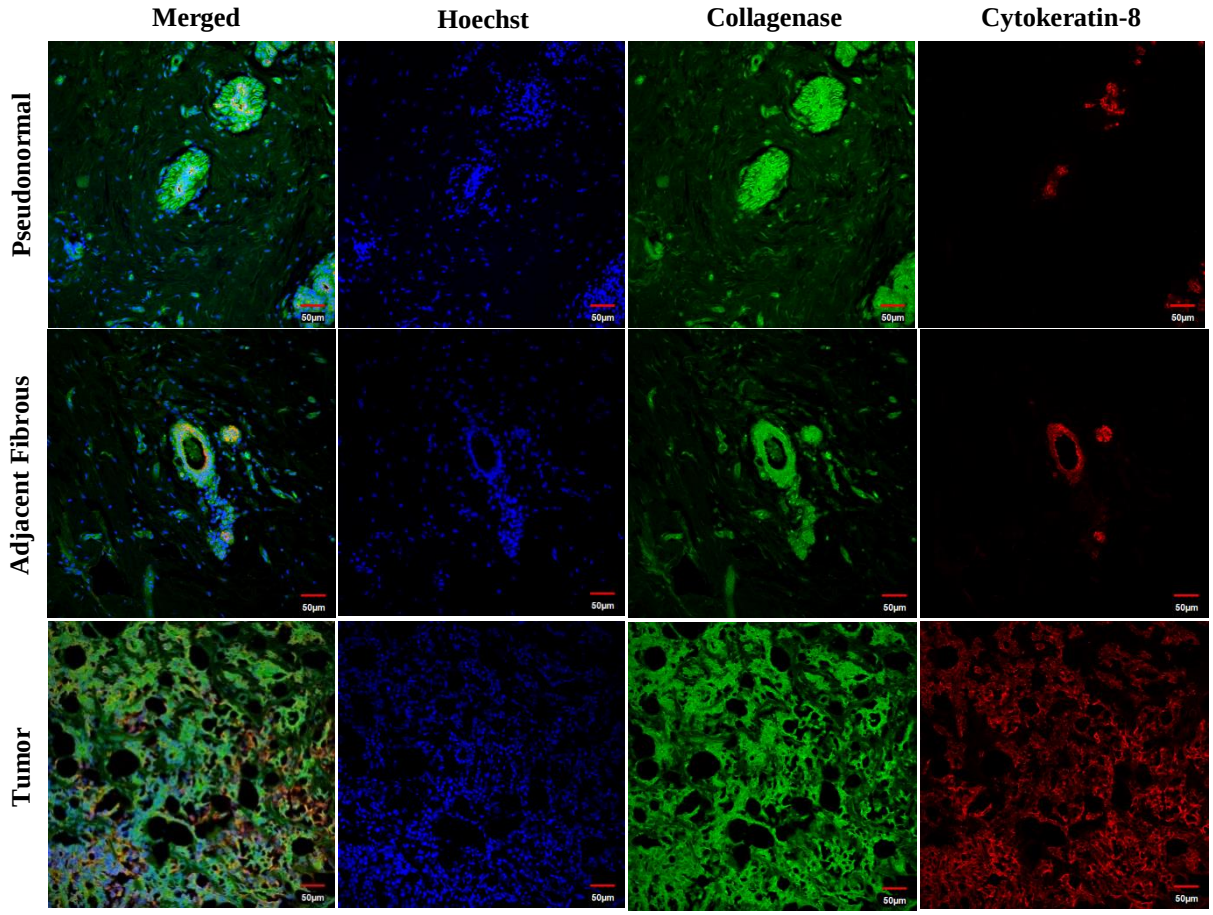

Figure 3-14 ZBF-fixed human tissue of breast tumor, adjacent fibrous tissue, and pseudonormal tissue (taken at least 2 cm away from tumor) stained for collagenase (green), the DNA-dye Hoechst (blue), and the epithelial cell antigen cytokeratin-8 (red), n=1. Scale bar = 50 µm. Images taken at 20x.

4. Conclusions

Pten -/- murine mammary fibroblasts were determined to have significantly higher MMP collagenase activity normalized to cell viability than wildtype murine mammary fibroblasts. Rheology was used to characterize elastic moduli of PEG-hydrogels ranging in stiffness from 0.75-6.21 kPa. Although results characterizing MMP activity normalized to metabolic activity of the wildtype and Pten -/- mammary fibroblasts encapsulated in PEG-hydrogels of varyng stiffness were found to be insignificant with large variability, metabolic activity remained consistently high with low variability between experiments. We are unsure what the cause of large variability in MMP activity normalized to metabolic activity is.

The MMP-collagenase substrate developed by Leight et al (2013) was found to be compatible with the ZBF fixation method developed by Hadler-Olsen et al (2010) allowing for precise localization of MMP collagenase activity. The MMP-collagenase peptide specificity for MMP-collagenase was further characterized and confirmed through the use of controls including autofluorescence, MMP activity inhibition, and temperature.

In situ zymography using the MMP-collagenase peptide was found to be compatible with immunohistochemistry. In situ zymography was combined with immunohistochemistry on human breast tissue to stain for collagenase activity and epithelial cells. Pseudonormal and fibrous tissue adjacent to the tumor showed similarities in normal epithelial duct and tissue morphology as well as greater levels of MMP collagenase activity localized to the epithelial ducts. Tumor tissue presented with

disorganized epithelial structure and greater MMP collagenase activity levels dispersed throughout the tissue.

5. Future Direction

Further investigation into the role of matrix stiffness in regulating MMP activity within the tumor microenvironment would include studying different cell lines of cell types residential to the tumor stroma such as epithelial cells, macrophages, and adipocytes.

A recent study found the MMP-9 activity in tumors was significantly associated to shortened disease-free survival and to relapse in patients with adenocarcinoma (Lee et al, 2015). Development of MMP peptide substrates specific to MMP9 could allow for staining of patient tumor biopsies and determination of prognostic factors. These MMP substrates could also be utilized in vitro with isolated cells to determine MMP activity produced that would correlate to a poor prognosis. Development of many MMP specific substrates with varying fluorophores would allow for staining and quantification of multiple kinds of MMP activity in vitro in both in situ zymography and PEG-hydrogel studies.

Elastography techniques have recently been developed to image soft tissue in vivo to measure the elastic modulus of tumors. This quantitative alternative to manual palpation can detect smaller, deeper tumors and quantify tissue stiffness (Samani et al, 2007). Quasi-static elastography uses ultrasound to create strain images used to approximate modulus distribution of the tissue (Samani et al, 2007). This method could be applied to tissues given to the Leight lab before fine needle aspiration or biopsy. Characterizing this elastic modulus of tissues before removal would allow for known tissue stiffness of samples stained using in situ zymography and immunohistochemistry and could correlate MMP activity seen in tissue sections to MMP activity of isolated cells from the same sample in different matrix stiffnesses in vitro.

6. References

Beckstead, J. (1994). A Simple Technique for Preservation of Fixation-sensitive Antigens in Paraffin-embedded Tissues. *The Journal of Histochemistry and Cytochemistry*. 42(8): 1127-1134.

Blanpain, C., & Fuchs, E. (2014). Plasticity of epithelial stem cells in tissue regeneration. Science (New York, N.Y.), 344(6189), 1242281. http://doi.org/10.1126/science.1242281

Bryan et al. (2013). The Clinical Breast Exam: A Skill that Should Not Be Abandoned. *Journal of General Internal Medicine*, 28(5), 719–722. http://doi.org/10.1007/s11606-013-2373-9

Colpaert et al. (2001). The Presence of a Fibrotic Focus Is an Independent Predictor of Early Metastasis in Lymph Node-Negative Breast Cancer Patients. *American Journal of Surgical Pathology*, 25(12: 1557-8.

Deryugina et al. (2006). Matrix Metalloproteinases and Tumor Metastasis. *Cancer Metastasis Review*, 25(1): 9-34.

Duraiyan et al. (2012). Applications of immunohistochemistry. *Journal of Pharmacy & Bioallied Sciences*, 4(Suppl 2), S307–S309. http://doi.org/10.4103/0975-7406.100281

George et al. (2010). In Situ Zymography. *Methods in Molecular Biology*. 622: 271-277.

Gialeli et al. (2010). Role of Matrix Metalloproteinases in Cancer Progression and their Pharmacological Targeting. *Federation of European Biochemical Societies Journal*. 278(2011): 16-27.

Goh et al. (2013). Electrodeposition of Lead-free Solder Alloys. *Soldering and Surface Mount Technology*. 25(2): 76-90.

Guidechem. Zinc(2+),(1,10-phenanthroline-kN1,kN10)-(CAS No. 16561-55-0). www.guidechem.com/reference/dic-417427. Accessed 10 April 2017.

Hadler-Olsen et al. (2010). Gelatin In Situ Zymography on Fixed, Paraffin-embedded Tissue: Zinc and Ethanol Fixation Preserve Enzyme Activity. *The Journal of Histochemistry and Cytochemistry*. 58(1): 29-39.

Ingthorsson et al. (2016). Epithelial Plasticity During Human Breast Morphogenesis and Cancer Progression. Journal of Mammary Gland Biology and Neoplasia, 21(3), 139–148. http://doi.org/10.1007/s10911-016-9366-3

Ismail et al. (2003). Immunohistologic Labeling of Murine Endothelium. *Cardiovascular Pathology*. 12(2): 82-90.

Klein et al. (2011). Physiology and Pathophysiology of Matrix Metalloproteinases. *Amino Acids*. 41(2): 271-290.

Lee et al. (2015). Prognostic effect of matrix metalloproteinase-9 in patients with resected Non small cell lung cancer. *Journal of Cardiothoracic Surgery*, *10*, 44. http://doi.org/10.1186/s13019-015-0248-3

Leight et al. (2017). Extracellular Matrix Remodeling and Stiffening Modulate Tumor Phenotype and Treatment Response. *Annual Review of Cancer Biology*. 2017.1: 313-334.

Leight et al. (2015). Multifunctional Bioscaffolds for 3D Culture of Melanoma Cells Reveal Increased MMP Activity and Migration with BRAF Kinase Inhibition.

Proceedings of the National Academy of Sciences of the United States of America. 112(17): 5366-71.

Leight et al. (2013). Direct Measurement of Matrix Metalloproteinase Activity in 3D Cellular Microenvironments Using a Fluorogenic Peptide Substrate. *Biomaterials*. 34(30): 7344-7352.

Levental et al. M. (2009). Matrix Crosslinking Forces Tumor Progression by Enhancing Integrin signaling. *Cancer Cell*, 139(5), 891–906. http://doi.org/10.1016/j.cell.2009.10.027

Luke et al. (1999). Matrix Metalloproteinase-9/Gelatinase B Is Required for Process Outgrowth by Oligodendrocytes. *Journal of Neuroscience*. 19 (19): 8464-8475.

National Center for Biotechnology Information. PubChem Compound Database; CID=1318, https://pubchem.ncbi.nlm.nih.gov/compound/1318 (accessed Apr. 11, 2017).

National Center for Biotechnology Information. PubChem Compound Database; CID=6049, https://pubchem.ncbi.nlm.nih.gov/compound/6049 (accessed Apr. 11, 2017).

Nguyen et al. (2016). Matrix Metalloproteinase Expression in the Rat Myometrium During Pregnancy, Term Labor, and Postpartum. *Biology of Reproduction*. 95(1): 1-14.

Nyborg et al. (2004). That zincing feeling: the effects of EDTA on the behaviour of zinc-binding transcriptional regulators. *Biochemical Journal*, 381(Pt 3), E3.

Painter et al. (2010). Useful Immunohistochemical Markers of Tumor Differentiation. *Toxicologic Pathology*, 38(1), 131–141. http://doi.org/10.1177/0192623309356449

Patricia et al. (2005). Zymographic Techniques for the Analysis of Matrix Metalloproteinases and Their Inhibitors. *Biotechniques*. 38: 73-83.

Paszek et al. (2005). Tensional Homeostasis and the Malignant Phenotype. *Cancer Cell*, 8(3): 241-254.

Radisky et al. (2010). Matrix Metalloproteinase-Induced Epithelial-Mesenchymal Transition in Breast Cancer. *Journal of Mammary Gland Biology and Neoplasia*, 15(2), 201–212. http://doi.org/10.1007/s10911-010-9177-x

Reya et al. (2001) Stem cells, cancer, and cancer stem cells. *Nature*, 414(6859): 105-111. http://hdl.handle.net/2027.42/62862

Samani et al. (2007). Elastic Moduli of Normal and Pathological Human Breast Tissues: an Inversion-Technique-Based Investigation of 169 Samples. *Physics in Medicine and Biology*. 52(6):1565-1576.

Trimboli et al. (2010). Pten in Stromal Fibroblasts Suppresses Mammary Epithelial Tumors. *Nature*. 461(7267): 1084-1091.

Verma et al. (2007). Matrix Metalloproteinases (MMPs): Chemical-biological functions and (Q)SARs. *Bioorganic and Medicinal Chemistry*, 15(6): 2223-2268.